American Mineralogist, Volume 101, pages 1483–1488, 2016

High-pressure behavior of the polymorphs of FeOOH

Mary M. Reagan[1,*], Arianna E. Gleason[2], Luke Daemen[3], Yuming Xiao[4], and Wendy L. Mao[1,5]

[1]Department of Geological Sciences, Stanford University, Stanford, California 94305, U.S.A.
[2]Shock and Detonation Physics, LANL, Los Alamos, New Mexico 87545, U.S.A.
[3]Spallation Neutron Source, Oak Ridge National Laboratory, Oak Ridge, Tennessee 37830, U.S.A.
[4]Advanced Photon Source, Argonne National Laboratory, Lemont, Illinois 60439, U.S.A.
[5]Photon Science, SLAC National Accelerator Laboratory, Menlo Park, California 94025, U.S.A.

Abstract

The high-pressure structural and electronic behavior of α-, β-, and γ-FeOOH were studied in situ using a combination of synchrotron X-ray diffraction (XRD) and X-ray emission spectroscopy (XES). We monitored α-FeOOH by XES as a function of pressure up to 85 GPa and observed an electronic spin transition that began at approximately 50 GPa, which is consistent with previous results. In the γ-FeOOH sample, we see the initiation of a spin transition at 35 GPa that remains incomplete up to 65 GPa. β-FeOOH does not show any indication of a spin transition up to 65 GPa. Analysis of the high-pressure XRD data shows that neither β-FeOOH nor γ-FeOOH transform to new crystal structures, and both amorphize above 20 GPa. Comparing our EOS results for the β and γ phases with recently published data on the α and ε phases, we found that β-FeOOH exhibits distinct behavior from the other three polymorphs, as it is significantly less compressible and does not undergo a spin transition. A systematic examination of these iron hydroxide polymorphs as a function of pressure can provide insight into the relationship between electronic spin transitions and structural transitions in these OH- and Fe^{3+}-bearing phases that may have implications on our understanding of the water content and oxidation state of the mantle.

Keywords: Spin transitions, high-pressure studies, XES, FeOOH, XRD data

Introduction

Iron hydroxides, including FeOOH and its polymorphs, are common on the surface of the Earth, where they are abundant in soils, aquifers, and sediments. FeOOH has four polymorphs, three of which are naturally occurring: goethite (α-FeOOH), akaganeite (β-FeOOH), and lepidocrocite (γ-FeOOH). A fourth polymorph, ε-FeOOH, can be synthesized at high pressure (Bolotina et al. 2008; Gleason et al. 2008; Voigt et al. 1981). Goethite is the thermodynamically stable phase at ambient conditions, whereas akaganeite is rare and forms in Cl-rich environments like hot brines and rust in marine environments. Lepidocrocite occurs in rocks, soils, and rust and is often an oxidation product of Fe^{2+}. Their structures consist of corner-linked double bands of $FeO_3(OH)_3$ octahedra (Fig. 1). α-FeOOH has double bands of edge sharing octahedra that form 2 × 1 channels. β-FeOOH also has double bands; however, they are arranged in a circular shape forming large 2 × 2 channels, which are stabilized by the presence of a variable molecule or ions such as H_2O, OH^-, Cl^-, or NO^{3-}. The γ-FeOOH bands are connected via hydrogen bonds (OH-O) and form corrugated 2D layers perpendicular to the *b*-axis. The high-pressure ε-FeOOH phase is a slightly distorted rutile structure with corner-linked single bands of edge-shared octahedra parallel to the *c*-axis (Otte et al. 2009). It is isostructural with δ-AlOOH, a phase that may transport hydrogen deep within the planet and potentially down to the core-mantle boundary (Sano et al. 2004; Suzuki 2010).

Based on crystal field theory, the distribution of electrons in the *d* orbitals in transition metal complexes depends on the ligand field geometry and the metal *d*-electron configurations. The spin state of iron is determined by the difference between the energy levels of Δ_c (the crystal field splitting parameter) and the spin pairing energy (Λ). Under ambient conditions, Δ_c for most octahedrally coordinated iron compounds is lower than Λ. This results in favorable energetic conditions where 3*d* electrons occupy both the t_{2g} orbitals and the higher energy e_g orbitals with unpaired spins. With increasing pressure, the crystal field splitting energy increases with respect to the spin pairing energy. This can result in the spin pairing of the electrons in the lower energy t_{2g} orbital. The spin transitions of iron in lower mantle minerals may result in significant changes in their physical and chemical properties (Speziale et al. 2005)—including their density, bulk modulus, seismic velocities, electrical conductivity, radiative heat transfer, and element partitioning (Lin et al. 2013, 2008, 2007; Speziale et al. 2005; Stackhouse et al. 2007). Previous work (Gleason et al. 2013; Xu et al. 2013) showed that spin transitions take place in α-FeOOH and ε-FeOOH. Gaining insight into the high-pressure behavior and spin state of the polymorphs of FeOOH can improve our understanding of more complex hydrogen bearing compounds that may be common in the Earth's deep interior (Williams and Hemley 2001).

Experimental methods

Sample synthesis

α-, β-, and γ-FeOOH were synthesized using the methods in Schertmann (2000). β-FeOOH was prepared following a slight modification. After dissolving

* E-mail: mreagan@stanford.edu

0003-004X/16/0006–1483$05.00/DOI: http://dx.doi.org/10.2138/am-2016-5449

54.6 g $FeCl_3 \cdot 6H_2O$ (0.2 mol) in 200 mL of deionized water in a 500 mL polyethylene bottle, a solution of 6 g NaOH in 120 mL deionized water was added to the iron chloride solution. A brown precipitate forms that redissolves upon shaking. The resulting clear, brown solution is allowed to age at room temperature for 3 days, at which point 40 mL of a 10 M solution of NaOH in deionized water is added rapidly with vigorous stirring. The resulting solution is heated to 80 °C in the closed polyethylene bottle until a brown precipitate starts appearing. This requires 6 to 7 days. After the solution becomes a cloudy suspension, heating is continued for 4 days. The suspension of β-FeOOH is difficult to filter by conventional means and the solid is separated from the supernatant liquid by centrifugation. The solid is washed repeatedly by resuspension in 250 mL of water, stirring for several minutes, and centrifugation. This washing operation is repeated several times until the supernatant liquid no longer gives a positive test for chloride by precipitation with a silver nitrate solution. The solid material is then dried in a vacuum oven at 40 °C.

Chloride analysis

The simplest method for chloride determination is Mohr titration with aqueous silver nitrate, using sodium chromate as an indicator (Skoog et al. 1996). The method requires to bring β-FeOOH in solution. Hydrochloric acid dissolves β-FeOOH quite readily, but, obviously, cannot be used for the sample preparation in the determination of chloride in β-FeOOH. Furthermore, any Broensted acid used to dissolve β-FeOOH cannot introduce an anion that forms an insoluble salt with silver. Nitric acid would be ideal, but does not dissolve β-FeOOH at or above room temperature. Sample preparation proceeded as follows. A small amount of β-FeOOH (ca. 50 mg) was placed in the polytetrafluoroethylene (Teflon) liner of a 23 mL Parr autoclave. Deionized water (8 mL) was placed in the vessel, then 4 mL of concentrated nitric acid. Four drops of triflic acid were added, after which the autoclave was sealed and placed in an oven. The temperature was raised progressively to 180 °C over a period of one day and the autoclave was kept at this temperature for two more days. The autoclave was allowed to cool down to room temperature before opening. The polytetrafluoroethylene liner contained a clear liquid with no visible traces of solid. This method of sample preparation has the advantage of preventing any loss of chlorine in the form of HCl. The clear solution was transferred to a 250 mL beaker, diluted with 100 mL of water, and pH was raised to about 6 with the addition of small amounts of sodium bicarbonate. At this pH, iron precipitates as iron hydroxide. This solid is filtered, washed carefully, and the filtrate is then used for Mohr titration with a 20 mM aqueous solution of silver nitrate. Three samples were prepared in this fashion for chloride determination. If a nominal formula for β-FeOOH is assumed to be $FeO(OH) \times Cl(1 - x)$, then the titration results gave $x = 0.84 \pm 0.015$, which indicates that some 15% of the hydroxide ions are replaced by chloride ions in the β-FeOOH structure. This is consistent with previous observations.

Sample preparation

Powdered samples of synthesized α-FeOOH, β-FeOOH, and γ-FeOOH (Gerth 1990; Kosmulski et al. 2003; Wang et al. 2004) were loaded separately into a beryllium (for XES), or tungsten or stainless steel (for XRD) gasket. For α-FeOOH, a 100 μm hole served as the sample chamber while a sample chamber of 120 μm was used for β-FeOOH and γ-FeOOH. All samples were compressed between 300 μm diamond culets in a symmetric diamond-anvil cell (DAC). No pressure-transmitting medium was used for the XES experiments to maximize signal, and silicone oil was used for the XRD experiments. Ruby and gold (Mao et al. 1978; Heinz et al. 1984) were used as pressure calibrants for the XRD experiments, while ruby only was used for the XES experiments.

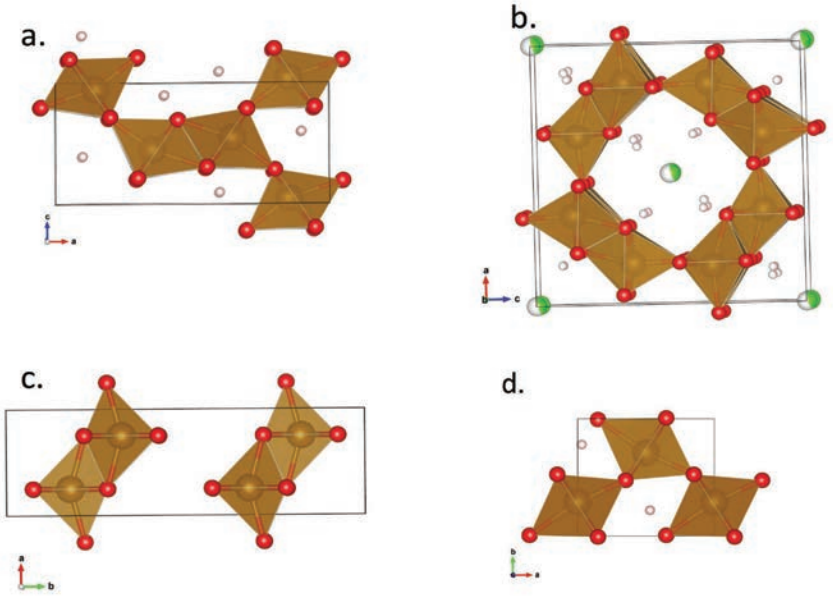

Figure 1. The ambient-pressure crystal structures of the FeOOH polymorphs showing iron (gold), oxygen (red), hydrogen (light pink), chlorine (green), and $FeO_3(OH)_3$ octahedra (tan). (**a**) α-FeOOH (goethite), (**b**) β-FeOOH (akaganeite), (**c**) γ-FeOOH (lepidocrocite), and (**d**) ε-FeOOH. These structures were generated using VESTA (Momma et al. 2008). (Color online.)

Table 1. A comparison of the experiments performed in this study

Phase	Technique (Beamline)	Specifications			Highest pressure (GPa)
		Gasket	Pressure medium	X-ray wavelength/energy	
α	XES (16-IDD, APS)	Be	None	11.3 keV	85
β	XES (16-IDD, APS)	Be	None	11.3 keV	65
β	XRD (16-BM-D, APS; 12.2.2 ALS)	Stainless steel	Silicone oil	0.4133 Å / 0.4246 Å	29
γ	XES (16-IDD, APS)	Be	None	11.3 keV	64
γ	XRD (12.2.2, ALS)	W	Silicone oil	0.4246 Å	34

Synchrotron X-ray experiments

Angle-dispersive powder XRD measurements were performed at beamline 12.2.2 of the Advanced Light Source (ALS), Lawrence Berkeley National Laboratory (LBNL), and at HP-CAT, beamline 16-BM-D at the Advanced Photon Source (APS), Argonne National Laboratory (ANL). At ALS, experiments had X-rays with a wavelength of 0.4959 Å, a beam spot of 10 × 10 μm, and a sample to detector distance of 354.41 mm. Experiments at APS had X-rays with a wavelength of 0.4246 Å, a beam spot size of 5 × 5 μm and a sample to detector distance of 320.66 mm. XRD data for β-FeOOH was collected at APS, while data for γ-FeOOH was collected at ALS. All data were collected on a MAR345 image plate and cell-parameter refinements were carried out using the MAUD program (Lutterotti et al. 1997). The Fe*K*β XES spectra of α-, β-, and γ-FeOOH were collected at HP-CAT, beamline 16ID-D, APS, ANL. The incident X-ray energy were monochromatized using a Si(111) double crystal monochromator and was centered at 11.3 keV, and the scans were set relative to 7.058 keV with a range of –40 to +25 eV. Table 1 provides a summary of the experimental techniques.

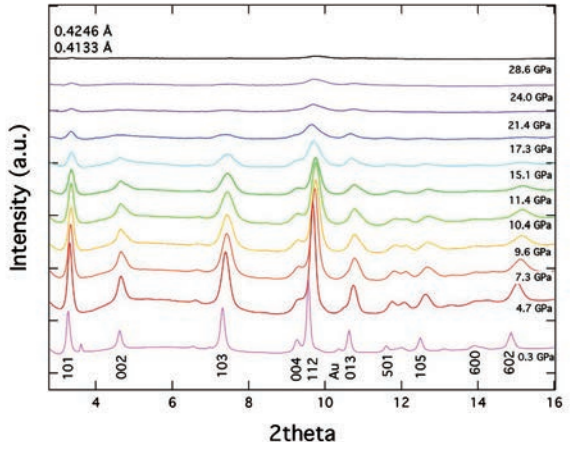

Figure 2. XRD spectra for β-FeOOH for selected pressures. The sample becomes amorphous above ~17 GPa. λ = 0.4133 Å, 0.3 to 15.1 GPa, and 0.4246 Å above 17.3 GPa. (Color online.)

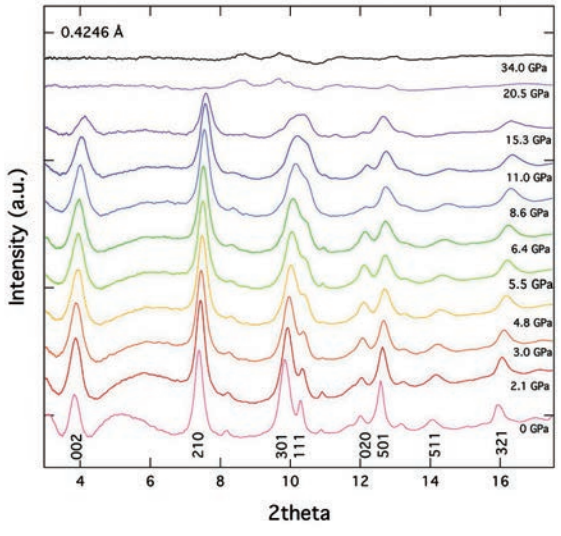

Figure 3. XRD spectra for γ-FeOOH for select pressures. It becomes amorphous above ~20 GPa. λ = 0.4246 Å. (Color online.)

Results

X-ray diffraction

The 2D patterns were integrated using Fit 2D (Hammersley 1998) and Le Bail refinements of the integrated patterns were carried out to determined the unit-cell volumes at each pressure using MAUD program (Lutterotti et al. 1997). Background fits were determined using a third-order polynomial that was manually set. Lattice parameters were refined to a goodness of fit of 0.6% (β) and 0.5% (γ) as determined by MAUD. For γ-FeOOH, the (200) peak was used to constrain the *a* lattice parameter at each pressure step. Analysis of the XRD data shows that neither β-FeOOH or γ-FeOOH undergo any first-order structural transitions over the pressure range studied, and both show evidence of amorphization above ~20 GPa (Figs. 2 and 3). We fit our pressure-volume data to a second-order Birch-Murnaghan equation of state (EOS) (Birch 1978), and found that β-FeOOH has a V_0 of 336.6(3) Å^3, and K_0 value of 284(1) GPa. The γ-FeOOH phase has a V_0 of 147.76(2) Å^3 and a K_0 value is 104(1) GPa. These results are summarized in Table 2 and plotted in Figures 4 and 5, where the β and γ phases are compared with recently published work on the α- and ε-phases (Xu et al. 2013 and Gleason et al. 2013, respectively).

X-ray emission spectroscopy

The spin state of iron is monitored through *K*β XES, where a *K* shell electron core-hole is created when an electron absorbs an X-ray photon and is emitted from the atom. This is followed by a 3*p* electron falling to the *K* shell, and in transition metals (e.g., iron), an exchange interaction occurs between the 3*p* core hole and the unpaired 3*d* shell when a material is in high spin. The resultant emission spectrum consists of $K\beta_{1,3}$ peak and the smaller satellite peak, *K*β′ that arises from the exchange interac-

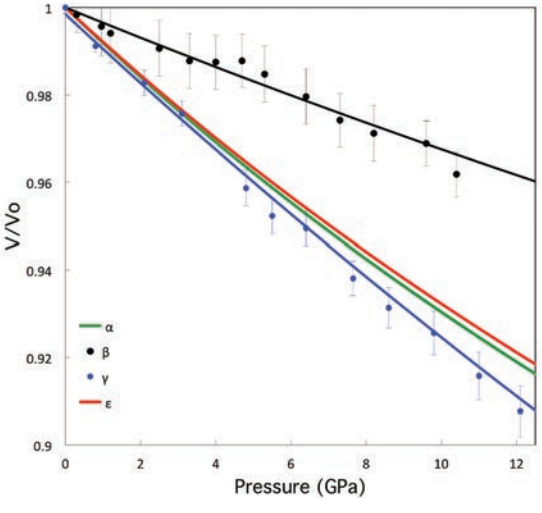

Figure 4. EOS for the FeOOH polymorphs. α and ε are plotted for comparison from previous published results (Xu et al. 2013; Gleason et al. 2008). Note the lower compressibility for β-FeOOH reflecting its higher *K* values. Both the β and γ phases become amorphous and their XRD spectra cannot be fit to a crystalline structure at higher pressures. (Color online.)

TABLE 2. A comparison of unit-cell volume, bulk modulus, and the spin transition pressure for the FeOOH polymorphs

Phase	V_0/f.u. (Å^3)	K_0 (GPa)	Spin transition pressure (GPa)
α[a]	34.6 (3)	120 (3)	49
β	42.1 (3)	283.6 (11)	N/A
γ	36.9 (2)	103.5 (10)	36
ε[b]	33.2 (5)	158 (5)	49

Notes: The pressure-volume data for all the phases were fit to a second-order Birch-Murnaghan equation of state.
[a] Xu et al. (2013).
[b] Gleason et al. (2008).

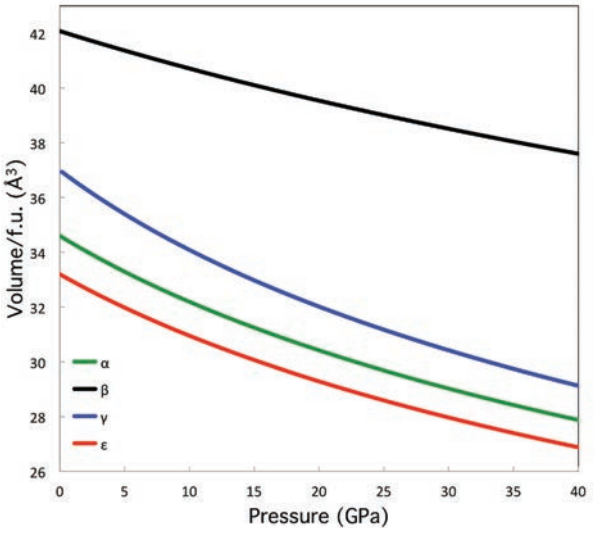

FIGURE 5. Volume per formula unit (f.u.) as a function of pressure. β-FeOOH has a significantly larger volume compared to the other three polymorphs. (Color online.)

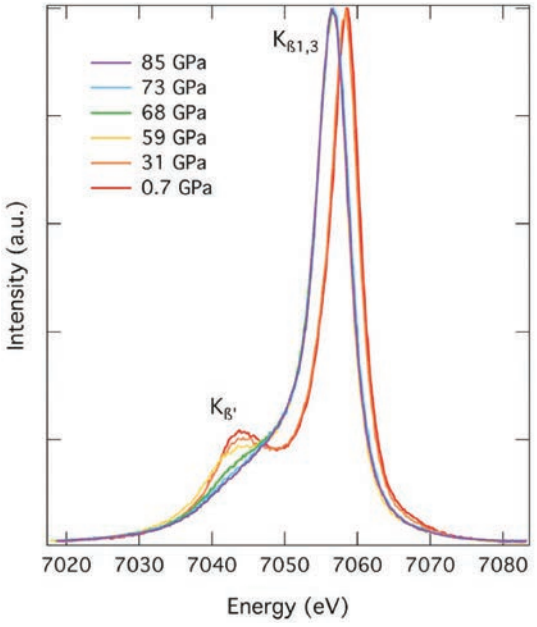

FIGURE 6. *K*β emission spectra as a function of pressure for α-FeOOH. (Color online.)

tion between 3*p* core hole and the 3*d* shell. We monitored α-FeOOH as a function of pressure up to 85 GPa and observed that it undergoes a spin transition beginning at ~50 GPa. This is seen in the evolution of the Kβ emission spectra where a clear reduction of Kβ′ was observed (Fig. 6). Each spectrum at a given pressure was summed and normalized using the integrated absolute difference method (IAD). The low spin state of α-FeOOH was used as the reference low-spin spectra for the calculations of the IAD of the β- and the γ-phases (Mattila et al. 2007). Our IAD values indicate the high to low spin transition occurred over a range of 50–70 GPa (Fig. 7). This is in good agreement with a previous study that found a high to low spin crossover above 45 GPa (Xu et al. 2013). In the γ-FeOOH sample, we see a spin transition beginning at 35 GPa that remains incomplete to 65 GPa, which is evidenced by the partial reduction of the satellite peak (Fig. 8). The β-FeOOH sample does not show any indication of a spin transition for pressures up to the highest pressure investigated, 65 GPa (Fig. 9). We note that although both the β and the γ phases become amorphous at pressures above 20 GPa, the study of the spin state provides valuable information about the electronic configuration despite the loss of the long-range order.

DISCUSSION

At ambient pressure, the polymorphs of FeOOH are made up of asymmetric octahedra of $Fe^{3+}_{HS}(O_1\text{-}H)_3(O_2\cdots H)_3$, with two distinct types of oxygen bonding, the shorter O_1-H and the longer $O_2\cdots H$. These bond lengths vary as they are subjected to pressure, with the length of the Fe-O_1 and Fe-O_2 bonds and the $O_1\cdots O_2$ distance affecting the spin state. These previous studies (Xu et al. 2013) have also linked the electronic spin transition with the

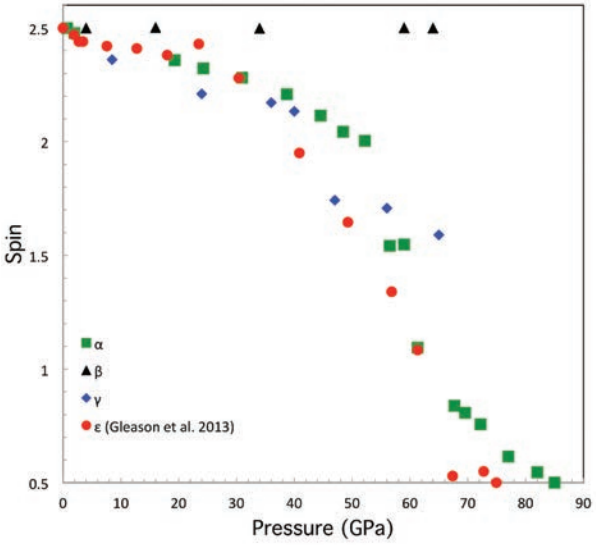

FIGURE 7. Average spin number as a function of pressure for α-FeOOH (green squares), β-FeOOH (black triangles), γ-FeOOH (blue diamonds) using the IAD method (Mattila et al. 2007). The low spin state for α-FeOOH was used to calculate the IAD values for β-FeOOH and γ-FeOOH. ε-FeOOH XES data from Gleason et al. (2013) was added (red circles). The spin transition for α-FeOOH begins at ~50 GPa. (Color online.)

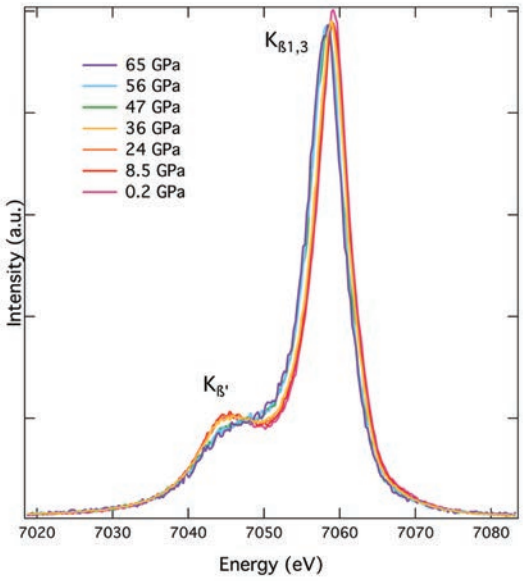

Figure 8. *K*β emission spectra as a function of pressure for γ-FeOOH. (Color online.)

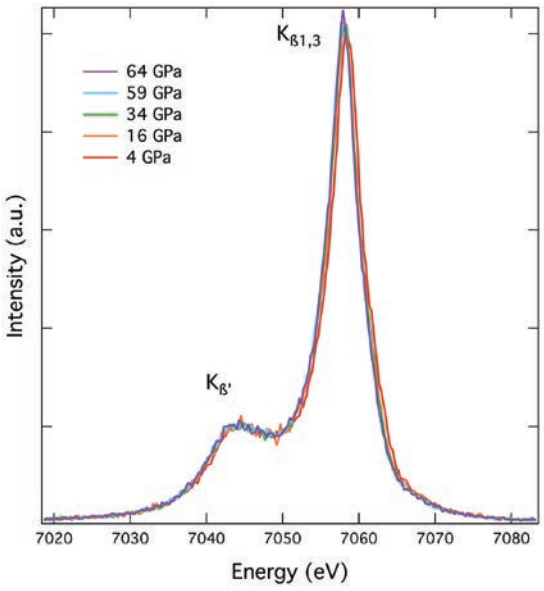

Figure 9. *K*β emission spectra as a function of pressure for β-FeOOH. (Color online.)

symmetrization of the hydrogen bonds in α-FeOOH. Increasing pressure leads to a shift in the proton position where the O_1-H and $O_2\cdots$H bonds become more equal in length. Single-crystal studies show that at 45 GPa, there is a large drop in volume that corresponds to a reduction of the Fe^{3+} radius (Xu et al. 2013). The asymmetry of the polyhedra is reduced as the Fe-O_1 and Fe-O_2 bonds are close to equal and the O_1-Fe-O_2 angle becomes 180°. α-FeOOH undergoes a spin transition at 47 GPa, with hydrogen bond symmetrization occurring at pressures above 50 GPa. In this case, the spin crossover leads to the hydrogen bond symmetrization (Xu et al. 2013). ε-FeOOH's behavior shows an opposite order of events, with increasing pressure: the spin transition starts at 49 GPa, while DFT calculations show that its hydrogen bonds symmetrize at a lower pressure of 43 GPa. The hydrogen bond symmetrization results in the elongation of the O_1-H and the compression of $O_2\cdots$H, with hydrogen reaching an equidistant position at ~1.2 Å and the O_1-H$\cdots O_2$ bond angle adjusting to 180° (Gleason et al. 2013). Interestingly, previous DFT calculations show that in γ-FeOOH the O_1-H remain constant at ~1.2 Å, while at 15 GPa, the $O_2\cdots$H bond reduces from 3.1 to 2.9 Å (Otte et al. 2009). Its spin transition begins at higher pressure of 36 GPa where the sample is amorphous and remains incomplete up to 65 GPa, the highest pressure we studied (Fig. 8). Previous DFT calculations for β-FeOOH, indicate that its O-H bonds remain nearly constant with increasing pressure up to 20 GPa (Otte et al. 2009). The DFT calculations for the β and γ phases only go up to 20 GPa, so it is not known how their bond lengths are changing at higher pressures, or at the onset of the spin transition in γ-FeOOH.

The β phase has a distinct behavior when compared to the other polymorphs of FeOOH. It is the only polymorph that does not undergo an electronic spin transition over the range of pressures studied. DFT calculations for β-FeOOH show that its oxygen-hydrogen bonds remain constant with increasing pressure. It is significantly less compressible as indicated by its higher K_0 value compared to the other polymorphs (Table 2). Its electronic configuration remaining in high spin maybe related to its incompressibility thus leading to polyhedra remaining more asymmetric and less compressed. There is small amount of Cl^- present in the β-FeOOH that stabilizes the 2 × 2 channels in its structure and is therefore less compressible allowing it to remain in the high-spin state with increasing pressure. β-FeOOH and to a lesser extent γ-FeOOH also have a larger volume per formula unit when compared with α- and ε-FeOOH (Table 2, Fig. 4). This may also contribute to why both β- and γ-FeOOH become amorphous at high pressure as they are energetically less stable than their denser polymorphs but the transition is hindered until they become mechanically unstable and amorphize. Future computational work to look at the hydrogen bonding as a function of pressure for β- and γ-FeOOH would provide further insight into the high-pressure behavior of these polymorphs.

Implications

It has been proposed that the electronic transition in Fe^{3+} and the symmetrization of the hydrogen bond are closely connected for the FeOOH polymorphs (Gleason et al. 2013; Xu et al. 2013). The spin transition is driven by the decreasing Fe-$O_{1,2}$ bonds and the change in the $O_1\cdots O_2$ distance, which leads to an environment that increases the crystal field splitting parameter until it is more energetically favorable for the low spin state. In full spin transitions, this change is often accompanied by the hydrogen bond symmetrization. In both α-FeOOH and ε-FeOOH, a complete spin transition is coupled with hydrogen bond symmetrization. In γ-FeOOH, there is only a partial shift in its hydrogen atom, which maybe a reflection that the polymorph does not undergo a full spin transition. β-FeOOH also shows this connection with

its bond length remaining relatively unchanged and a lack of a spin transition. Hydrogen bond symmetrization has also been observed at high pressure in α-AlOOH, which is isostructural with α-FeOOH and is present in subducting sedimentary rocks. Its hydrogen bonds become increasingly more symmetric up through the studied range of 50 GPa (Friedrich et al. 2007). Other oxy-hydroxide transition metal compounds may also undergo hydrogen bond symmetrization when subjected to high pressure, and further work is needed to understand the possible connection between hydrogen bond symmetrization and electronic structure changes. The symmetrization of hydrogen bonds is expected to have an effect on the elasticity and plasticity of hydrogen-bearing materials. Quantifying the high-pressure behavior of the hydrogen bonds in relation to hydrous Fe-bearing minerals with the potential for undergoing an electronic transition can give insight into the behavior of hydrogen in an Fe-rich environment at deep Earth conditions (Benoit et al. 1998; Gilli et al. 2009; Friedrich et al. 2007; Holzapfel 1972; Xu et al. 2013).

Iron is the most abundant transition metal in the deep Earth, and iron-bearing materials may transition to a low spin state at shallower depths as their water content increases (Frost and McCammon 2008; Otte et al. 2009; Xu et al. 2013). The experimental work on the polymorphs of FeOOH indicate that increasing pressure can have dramatic effects on the electronic state and the crystal structure, including the nature of the hydrogen bonds. This effect may be ubiquitous in transition metal bearing compounds that contain water and are relevant to the deep Earth. Ferric iron bearing silicates may play an important role in transporting water into the deep mantle. Changes to their spin states and hydrogen bonds might then have an influence on the water dynamics and balance within the deep Earth (Williams and Hemley 2001). This has implications for the oxidation state of the Earth's mantle, where the redox state controls Fe^{3+} and OH^- content within minerals, as well as, water partitioning in fluids/melts and minerals (Frost and McCammon 2008).

Acknowledgments

M.M. Reagan, A.E. Gleason, and W.L. Mao are supported by the NSF Geophysics Program (EAR-1446969). We thank Paul Chow (APS), Alastair MacDowell (ALS), and Jinyuan Yan (ALS) for their assistance with the synchrotron experiments, and Jinfu Shu (Geophysical Lab) for help with sample loading. Portions of this work were performed at beamline 12.2.2 of ALS, LBNL. ALS is supported by the Director, Office of Science, Office of Basic Energy Sciences (BES), of the U.S. Department of Energy (DOE) under Contract No. DE-AC02-05CH11231. Portions of this work were also performed at HPCAT (Sector 16), APS, ANL. HPCAT operations are supported by DOE-NNSA under Award No. DE-NA0001974 and DOE-BES under Award No. DE-FG02-99ER45775, with partial instrumentation funding by NSF. APS is a DOE-BES User Facility operated for the DOE Office of Science by ANL under Contract No. DE-AC02-06CH11357.

References cited

Benoit, M., Marx, D., and Parrinello, M. (1998) Tunnelling and zero-point motion in high-pressure ice. Nature, 392, 258–261.

Birch, F. (1978) Finite strain isotherm and velocities for single-crystal and polycrystalline NaCl at high pressures and 300°K. Journal of Geophysical Research, 83, 1257–1268.

Bolotina, N., Molchanov, V., Dyuzheva, T., Lityagina, L., and Bendeliani, N. (2008) Single-crystal structures of high-pressure phases FeOOH, FeOOD, and GaOOH. Crystallography Reports, 53, 960–965.

Friedrich, A., Haussül, E., Boehler, R., Morgenroth, W., Juarez-Arellano, E.A., and Winkler, B. (2007) Single-crystal structure refinement of diaspore at 50 GPa. American Mineralogist, 92, 1640–1644.

Frost, D.J., and McCammon, C.A. (2008) The redox state of Earth's mantle. Annual Review of Earth and Planetary Sciences, 36, 389–420.

Gerth, J. (1990) Unit-cell dimensions of pure and trace metal-associated goethites. Geochimica et Cosmochimica Acta, 54, 363–371.

Gilli, G., and Gilli, P. (2009) The Nature of the Hydrogen Bond. Oxford University Press, New York.

Gleason, A.E., Jeanloz, R., and Kunz, M. (2008) Pressure-temperature stability studies of FeOOH using X-ray diffraction. American Mineralogist, 93, 1882–1885.

Gleason, A.E., Quiroga, C.E., Suzuki, A., Pentcheva, R., and Mao, W.L. (2013) Symmetrization driven spin transition in ε-FeOOH at high pressure. Earth and Planetary Science Letters, 379, 49–55.

Hammersley, A.P. (1998) Fit2D: V99.129 Reference Manual Version 3.1. Internal Report ESRF-98-HA01.

Heinz, D., and Jeanloz, R. (1984) The equation of state of the gold calibration standard. Journal of Applied Physics, 55, 885–893.

Holzapfel, W.B. (1972) Symmetry of the hydrogen bonds in Ice VII. Journal of Chemical Physics, 56, 712–715.

Kosmulski, M., Maczka, E., Jartych, E., and Rosenholm, J.B. (2003) Synthesis and characterization of goethite and goethite-hematite composite: Experimental study and literature survey. Advances in Colloid and Interface Science, 103, 57–76.

Lin, J.F., and Tsuchiya, T. (2008) Spin transition of iron in the Earth's lower mantle. Physics of the Earth and Planetary Interiors, 170, 248–259.

Lin, J.F., Vankó, G., Jacobsen, S.D., Iota, V., Struzhkin, V.V., Prakapenka, V.B., Kuznetsov, A., and Yoo, C.-S. (2007) Spin transition zone in Earth's lower mantle. Science, 317, 1740–1743.

Lin, J.F., Speziale, S., Mao, Z., and Marquardt, H. (2013) Effects of the electronic spin transitions of iron in lower mantle minerals: Implications for deep mantle geophysics and geochemistry. Reviews of Geophysics, 51, 244–275.

Lutterotti, L., Matthies, S., Wenk, H.-R., Schultz, A.S., and Richardson, J.W. (1997) Combined texture and structure analysis of deformed limestone from time-of-flight neutron diffraction spectra. Journal of Appied Physics, 81, 594–600.

Mao, H.K., Xu, J., and Bell, P.M. (1978) High pressure physics: Sustained static generation of 1.36 to 1.72 megabars. Science, 200, 1145–1147.

Mattila, A., Pylkkänen, T., Rueff, J-P., Huotari, S., Vankó, G., Hanfland, M., Lehtinen, M., and Hämäläinen, K. (2007) Pressure induced magnetic transition in siderite $FeCO_3$ studied by X-ray emission spectroscopy. Journal of Physics, 19, 386206.

Momma, K., and Izumi, F. (2008) VESTA: a three-dimensional visualization system for electronic and structural analysis. Journal of Appied Crystallography, 41, 653–658.

Otte, K., Pentcheva, R., Schmahl, W.W., and Rustad, J.R. (2009) Pressure-induced structural and electronic transitions in FeOOH from first principles. Physical Review B, 80, 205116.

Sano, A., Ohtani, E., Kubo, T., and Funakoshi, K.I. (2004) In situ X-ray observation of decomposition of hydrous aluminum silicate $AlSiO_3OH$ and aluminum oxide hydroxide d-AlOOH at high pressure and temperature. Journal of Physics and Chemistry of Solids, 65, 1547–1554.

Skoog, D.A., West, D.M., and Holler, F.J. (1996) Fundamentals of Analytical Chemistry, 7th ed. Thomson, Belmont, California.

Speziale, S., Milner, A, Lee, V.E., Clark, S.M., Pasternak, M.P., and Jeanloz, R. (2005) Iron spin transition in Earth's mantle. Proceedings of the National Academy of Sciences, 102, 17918–17922.

Stackhouse, S., Brodholt, J.P., and Price, G.D. (2007) Electronic spin transitions in iron-bearing $MgSiO_3$ perovskite. Earth and Planetary Science Letters, 253, 282–290.

Suzuki, A. (2010) High-pressure X-ray diffraction study of ε-FeOOH. Physics and Chemistry of Minerals, 37, 153–157.

Schwertmann, U., and Cornell, R.M. (2000) The Iron Oxides in the Laboratory, 2nd ed. Wiley-VCH, Weinheim.

Voigt, R., and Will, G. (1981) The system Fe_2O_3-H_2O under high pressures. Neues Jahrbuch für Mineralogie, 2, 89–96.

Wang, X., Chen, X., Gao, L., Zheng, H., Ji, M., Tang, C., Shen, T., and Zhang, Z. (2004) Synthesis of β-FeOOH and α-Fe_2O_3 nanorods and electrochemical properties of β-FeOOH. Journal of Material Chemistry, 905–907.

Williams, Q., and Hemley, R. (2001) Hydrogen in the deep earth. Annual Review of Earth and Planetary Sciences, 29, 365–418.

Xu, W., Greenberg, E., Rozenberg, G.K., Pasternak, M.P., Bykova, E., Boffa-Ballaran, T., Dubrovinsky, L., Prakapenka, V., Hanfland, M., Vekliova, O., and others. (2013) Pressure-induced hydrogen bond symmetrization in iron oxyhydroxide. Physical Review Letters, 111, 175501.

Manuscript received June 5, 2015
Manuscript accepted February 16, 2016
Manuscript handled by Sergio Speziale